

Ferromagnetic resonance in a current driven nanopillar

Joern N. Kupferschmidt, Shaffique Adam, and Piet W. Brouwer

Laboratory of Atomic and Solid State Physics, Cornell University, Ithaca, NY 14853-2501, USA

(Dated: May 25, 2019)

We present a theoretical analysis of current driven ferromagnetic resonance in a ferromagnet–normal-metal–ferromagnet tri-layer. This method of driving ferromagnetic resonance was recently realized experimentally by Tulapurkar *et al.* [Nature **438**, 339 (2005)] and Sankey *et al.* [Phys. Rev. Lett. **96**, 227601 (2006)]. The precessing magnetization rectifies the alternating current applied to drive the ferromagnetic resonance and leads to the generation of a dc voltage. Our analysis shows that a second mechanism to generate a dc voltage, rectification of spin currents emitted by the precessing magnetization, has a contribution to the dc voltage that is of approximately equal size for the thin ferromagnetic films used in the experiment.

PACS numbers: 76.50.+g,72.25.Ba,75.75.+a,85.75.-d

I. INTRODUCTION

A decade ago, Slonczewski¹ and Berger² predicted that a spin-polarized current passing through a ferromagnet exerts a torque on its magnetic moment. The past decade has shown an abundance of experiments that have confirmed this theoretical prediction.^{3,4,5,6,7} Since spin-polarized currents are easily generated by passing an electrical current through a ferromagnet, the ‘spin transfer torque’ opens the way for all-electrical manipulation of nanoscale magnetic devices.^{8,9}

Very recently, two groups have been able to use the spin torque to drive and detect ferromagnetic resonance in a ferromagnet–normal-metal–ferromagnet (FNF) trilayer.^{10,11} These experiments are designed such that the magnetization direction of one of the ferromagnets is fixed by anisotropy forces, whereas the other magnet is made of a softer ferromagnetic material or has a more symmetric shape so that its magnetization can more easily respond to the applied current or to an applied magnetic field. In both experiments, an alternating electrical current is used to drive the ferromagnetic resonance, whereas the magnetization precession is detected through the dc voltage generated by rectification of the applied ac current by the time-dependent resistance of the device.^{10,11} The theoretical analysis of this experimental setup is the subject of this article.

Not only does a spin-polarized current have an effect on the direction of the magnetization of a ferromagnet, a time varying magnetization also causes the flow of spin currents in normal metal conductors in electrical contact to the ferromagnet. This ‘spin emission’ was first proposed by Tserkovnyak, Brataas, and Bauer as the cause of enhanced damping of ferromagnetic resonance in thin ferromagnetic films in good electrical contact to a normal metal substrate.¹² Spin emission affects the experiments of Refs. 10 and 11 in two different ways. First, through the enhancement of the damping spin emission broadens the ferromagnetic resonance. Second, the free layer’s precessing magnetization emits alternating spin currents, which, in turn, generate a dc voltage through the time-varying spin-dependent conductance of the free

layer. That way, spin emission provides an alternative to rectification of the applied ac current as a mechanism for the generation of a dc voltage in these experiments. Our calculations show that both consequences of spin emission appear or disappear together: If spin emission gives a significant contribution to the damping of the ferromagnetic resonance — which is the case for the few nm-thick free-layer ferromagnets used in the experiments —, then it also provides a sizable contribution to the measured dc voltage, and vice versa.

In the remainder of this article we present the detailed theory of the electrical-current driven ferromagnetic resonance needed to arrive at the above conclusion. In addition, our theory allows us to calculate how the ferromagnetic resonance frequency, the resonance width, and the asymmetry of the resonance lineshape are affected by embedding the free ferromagnetic layer into the FNF trilayer. Our calculation proceeds in three parts. In Sec. II we derive general expressions for the spin transfer torque, which we then apply to the calculation of the magnetization motion in Sec. III. The generated dc voltage is calculated in Sec. IV. We conclude in Sec. V.

II. SPIN TRANSFER TORQUE

A schematic drawing of the system we consider is shown in Fig. 1. It consists of a ferromagnetic source reservoir, held at electric voltage V , a thin normal-metal spacer layer, a thin ferromagnetic layer, and a normal-metal drain reservoir. The direction \mathbf{n} of the magnetization in the ferromagnetic source is considered to be fixed, whereas the direction \mathbf{m} of the magnetization in the thin layer can change under the influence of an electrical current or an applied magnetic field.

The nonequilibrium spin transfer torque arises from the discontinuity of the spin current \mathbf{J}_s across the free ferromagnetic layer,^{1,13,14}

$$\boldsymbol{\tau}_{ne} = -[\mathbf{J}_s(+) - \mathbf{J}_s(-)], \quad (1)$$

where $\mathbf{J}_s(+)$ and $\mathbf{J}_s(-)$ are spin currents at the normal-metal–ferromagnet interfaces measured on the side of the

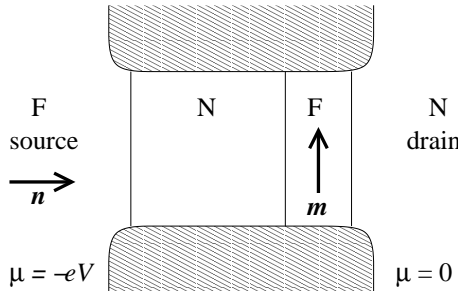


FIG. 1: Schematic drawing of the ferromagnet–normal-metal–ferromagnet trilayer considered here. The left ferromagnet, with magnetization direction \mathbf{n} , acts as the source reservoir. The right ferromagnet is the free layer. Its magnetization direction \mathbf{m} can change in response to the applied current. The currents $J(+)$ and $J(-)$ in the text are evaluated at the right and left sides of the free ferromagnetic layer, respectively.

drain reservoir and the spacer, respectively. We assume that the spacer layer and the free ferromagnet are sufficiently thin, so that all voltage drops occur across the ferromagnet–normal-metal interfaces.¹⁵ In that case, the charge currents $J_c(\pm)$ and the spin currents $\mathbf{J}_s(\pm)$ can be expressed directly in terms of the charge and spin accumulations μ_c and μ_s in the spacer layer. For the charge and spin currents $J_c(-)$ and $J_s(-)$ one has two sets of equations, one arising from the interface with the ferromagnetic source reservoir,^{8,9,16}

$$\begin{aligned} J_c(-) &= \frac{1}{e} [2G_+(\mu_c + eV) + 2G_-\mu_s \cdot \mathbf{n}], \\ \mathbf{J}_s(-) &= -\frac{\hbar}{2e^2} [2G_+\mu_s \cdot \mathbf{n} + 2G_-(\mu_c + eV)] \mathbf{n} \\ &\quad + \frac{\hbar}{2e^2} [2G_1(\mu_s \times \mathbf{n}) \times \mathbf{n} + 2G_2\mu_s \times \mathbf{n}], \end{aligned} \quad (2)$$

and one arising from the interface with the free ferromagnetic layer,^{8,9,12}

$$\begin{aligned} J_c(-) &= -\frac{1}{e} [g_+\mu_c + g_-\mu_s \cdot \mathbf{m}] \\ \mathbf{J}_s(-) &= \frac{\hbar}{2e^2} [g_-\mu_c + g_+\mu_s \cdot \mathbf{m}] \mathbf{m} \\ &\quad - \frac{\hbar}{2e^2} g_1 [2\mu_s \times \mathbf{m} + \hbar \dot{\mathbf{m}}] \times \mathbf{m} \\ &\quad - \frac{\hbar}{2e^2} g_2 [2\mu_s \times \mathbf{m} + \hbar \dot{\mathbf{m}}]. \end{aligned} \quad (3)$$

Here $G_\pm = (G_\uparrow \pm G_\downarrow)/2$ and $G_1 + iG_2 = G_{\uparrow\downarrow}$ are determined by the interface conductances for majority and minority electrons and by the mixing conductance for the interface between the ferromagnetic source and the normal-metal spacer, whereas $g_\pm = (g_\uparrow \pm g_\downarrow)/2$ and $g_1 + ig_2 = g_{\uparrow\downarrow}$ represent the equivalent quantities for the interface between spacer layer and the free ferromagnet and for the interface between the free ferromagnet and the source. Numerical values for these conductance coefficients have been obtained for the interfaces of

various combinations of ferromagnetic and normal-metal materials.¹⁷ The two sets of equations are slightly different because there are two ferromagnet–normal-metal interfaces between the spacer layer and the drain reservoir, whereas there is only one interface between the spacer layer and the source reservoir, see Fig. 1.¹⁸ Also, in Eq. (2), we omitted terms proportional to the time derivative $\dot{\mathbf{n}}$ because the magnetization of the source reservoir is held fixed. Similarly, for $J_c(+)$ and $\mathbf{J}_s(+)$ we find

$$\begin{aligned} J_c(+) &= -\frac{1}{e} [g_+\mu_c + g_-\mu_s \cdot \mathbf{m}] \\ \mathbf{J}_s(+) &= \frac{\hbar}{2e^2} [g_-\mu_c + g_+\mu_s \cdot \mathbf{m}] \mathbf{m} \\ &\quad + \frac{\hbar^2}{2e^2} g_1 \dot{\mathbf{m}} \times \mathbf{m} + \frac{\hbar^2}{2e^2} g_2 \dot{\mathbf{m}}. \end{aligned} \quad (4)$$

Note that the charge current J_c and the component $\mathbf{J}_s \cdot \mathbf{m}$ of the spin current parallel to the direction of the magnetization of the free layer are conserved.

Since G_2 and g_2 are numerically small for metallic junctions (20% or less of G_1 and g_1),^{17,19,20} we set G_2 and g_2 to zero in the following calculations. At the end of Sec. IV we discuss how our results are modified for finite G_2 and g_2 .

The flow of electrical current through the FNF trilayer generates a spin-transfer torque only if the magnetization directions \mathbf{n} and \mathbf{m} are not collinear. In the experiment of Refs. 10 and 11 this is achieved by an applied magnetic field which orients the free-layer magnetization \mathbf{m} at a finite angle with respect to the fixed-layer magnetization direction \mathbf{n} in the absence of a current. Following Ref. 11, we take this angle to be 90 degrees. We choose a right-handed set of coordinate axes $(\mathbf{e}_1, \mathbf{e}_2, \mathbf{e}_3)$ such that \mathbf{n} points along \mathbf{e}_1 and \mathbf{m} points along \mathbf{e}_3 if no current is applied. The application of a current will cause \mathbf{m} to deviate from \mathbf{e}_3 . We'll be interested in the linear response regime, in which the magnetization components m_1 and m_2 are proportional to the applied current J .

With an alternating current bias, $J_c = J(t) = \text{Re } J_0 e^{i\omega t}$, Eqs. (2) and (3) give five independent equations, from which one can solve for the five unknown variables, which are the charge and spin accumulations μ_c and μ_s in the spacer layer and the bias voltage V . Solving these to lowest order in the applied current, we find that two relevant components of the spin transfer torque (1) are

$$\tau_{\text{ne},1} = -\frac{\hbar}{2e} \left[J \frac{G_-}{G_{1+}} + \frac{\hbar m_2 g_1}{e} \left(2 - \frac{G_+}{G_{1+}} \right) \right], \quad (5)$$

$$\tau_{\text{ne},2} = \frac{\hbar}{2e} \frac{\hbar m_1 g_1}{e} \left(2 - \frac{g_1}{g_1 + G_1} \right), \quad (6)$$

where we abbreviated

$$G_{1+} = G_+ + (G_+^2 - G_-^2)/g_1. \quad (7)$$

III. MAGNETIZATION DYNAMICS

The magnetization is driven out of equilibrium by the spin transfer torque of Eq. (1). In order to solve for the full time-dependence of the magnetization, we use the Landau-Lifshitz-Gilbert equation,^{21,22}

$$\dot{\mathbf{m}} = \alpha \mathbf{m} \times \dot{\mathbf{m}} + \frac{\gamma}{Md} (\boldsymbol{\tau}_{\text{eq}} + \boldsymbol{\tau}_{\text{ne}}). \quad (8)$$

Here M is the magnetization per unit length, d is the thickness of the free ferromagnetic layer, γ is the gyro-magnetic ratio, and α is the phenomenological Gilbert damping parameter. The equilibrium torque $\boldsymbol{\tau}_{\text{eq}}$ is the combination of the torque applied by the external magnetic field and the anisotropy torque intrinsic to the ferromagnet. Since we are interested in small deviations from equilibrium, we can expand $\boldsymbol{\tau}_{\text{eq}}$ around the equilibrium direction $\mathbf{m} = \mathbf{e}_3$,

$$\boldsymbol{\tau}_{\text{eq}} = -\frac{Md}{\gamma} (\omega_1 m'_1 \mathbf{e}'_1 + \omega_2 m'_2 \mathbf{e}'_2) \times \mathbf{m}, \quad (9)$$

where the frequencies ω_1 and ω_2 are set by the energy cost for magnetization deviations along principal axes \mathbf{e}'_1 and \mathbf{e}'_2 perpendicular to \mathbf{e}_3 . The constants ω_1 and ω_2 depend on the dipolar field of the pinned layer, the demagnetization field and coercivity of the free layer, and the applied magnetic field.²³ The geometric mean $(\omega_1 \omega_2)^{1/2}$ is the free layer's ferromagnetic resonance frequency in the absence of electrical contact to the normal-metal spacer layer and the drain reservoir, whereas $(\omega_1 / \omega_2)^{1/2}$ is the ratio of semi-major and semi-minor axis of the ellipsoidal magnetization precession in that case. If $\boldsymbol{\tau}_{\text{eq}}$ is dominated by the applied magnetic field H , one has $\omega_1 = \omega_2 = \gamma H$. Rotating to the coordinate system with unit vectors \mathbf{e}_1 and \mathbf{e}_2 , the two components of $\boldsymbol{\tau}_{\text{eq}}$ can be written

$$\begin{aligned} \tau_{\text{eq},1} &= \frac{Md}{\gamma} [-m_2(\omega_+ + \omega_- \cos \phi) + m_1 \omega_- \sin \phi], \\ \tau_{\text{eq},2} &= \frac{Md}{\gamma} [m_1(\omega_+ - \omega_- \cos \phi) - m_2 \omega_- \sin \phi], \end{aligned} \quad (10)$$

where $\omega_{\pm} = (\omega_2 \pm \omega_1)/2$ and $\phi/2$ is the rotation angle between \mathbf{e}'_1 and \mathbf{e}_1 .

With an applied ac current, $J(t) = \text{Re } J_0 e^{i\omega t}$ we can then solve for the magnetization components $m_1(t) = \text{Re } m_{10} e^{i\omega t}$ and $m_2(t) = \text{Re } m_{20} e^{i\omega t}$, with the result

$$m_{10} = m_0 \frac{(J_0/e)(i\omega + \omega_- \sin \phi)}{f(\omega)}, \quad (11)$$

$$m_{20} = m_0 \frac{(J_0/e)(\omega_+ - \omega_- \cos \phi + i\omega(\tilde{\alpha}_+ + \tilde{\alpha}_-))}{f(\omega)}, \quad (12)$$

where we abbreviated

$$\begin{aligned} f(\omega) &= (1 + \tilde{\alpha}_+^2 - \tilde{\alpha}_-^2)\omega^2 - 2i\omega(\tilde{\alpha}_+ \omega_+ + \tilde{\alpha}_- \omega_- \cos \phi) \\ &\quad + \omega_-^2 - \omega_+^2, \end{aligned} \quad (13)$$

$$m_0 = \gamma \hbar G_- / 2dM G_{1+}, \quad (14)$$

and

$$\tilde{\alpha}_+ = \alpha + \frac{g_1 \gamma \hbar^2}{4de^2 M} \left(4 - \frac{G_+}{G_{1+}} - \frac{g_1}{g_1 + G_1} \right), \quad (15)$$

$$\tilde{\alpha}_- = \frac{g_1 \gamma \hbar^2}{4de^2 M} \left(\frac{G_+}{G_{1+}} - \frac{g_1}{g_1 + G_1} \right). \quad (16)$$

The non-negative dimensionless numbers $\tilde{\alpha}_{\pm}$ are the effective Gilbert damping parameters.¹² We need two damping parameters rather than one since the effective damping is anisotropic because of the presence of the second ferromagnet.

IV. DC VOLTAGE

Since we are interested in the dc voltage generated by the applied ac current, we need to calculate the voltage $V(t)$ to second order in $J(t)$. This implies that we need to solve Eqs. (2) and (3) to first order in m_1 and m_2 ,

$$\begin{aligned} V = J &\left(\frac{2G_1 + g_+}{G_1 g_{1+}} + \frac{G_+ + g_1}{2g_1 G_{1+}} \right) - \frac{\hbar \dot{m}_2 G_-}{2eG_{1+}} \\ &- \frac{2(g_1 + G_1)g_- G_- m_1}{G_1 g_1 g_{1+} G_{1+}} \left(J - \frac{e \dot{m}_2 \tilde{\alpha}_-}{m_0} \right), \end{aligned} \quad (17)$$

where we abbreviated

$$g_{1+} = 2g_+ + (g_+^2 - g_-^2)/G_1. \quad (18)$$

The two terms in the first line of Eq. (17), which are proportional to J and \dot{m}_2 , give an alternating contribution to V only. The term proportional to J is the dc resistance of the device, whereas the term proportional to \dot{m}_2 is the magnetic contribution to the admittance. (Electronic contributions to the admittance occur at higher frequencies than the ferromagnetic resonance frequency and are not considered in our theory.) The dc voltage follows from the sub-leading terms in the second line of Eq. (17), which are proportional to Jm_1 and $\dot{m}_2 m_1$. The contribution proportional to Jm_1 is rectification of the applied alternating current by the time-dependent conductance of the device. The contribution proportional to $\dot{m}_2 m_1$ follows from spin emission by the precessing magnetization of the free ferromagnet.

The two terms contributing to the dc voltage are easily calculated using the results of the previous section. Using Eqs. (11) and (12), one calculates the averages of the products Jm_1 and $\dot{m}_2 m_1$ over one period of the applied current,

$$\begin{aligned} \langle Jm_1 \rangle &= \frac{m_0 |J_0|^2}{2e|f(\omega)|^2} [\omega \text{Im } f(\omega) + \omega_- \sin \phi \text{Re } f(\omega)], \\ \langle \dot{m}_2 m_1 \rangle &= \frac{m_0^2 |J_0|^2 \omega^2}{2e^2 |f(\omega)|^2} \\ &\quad \times [\omega_+ - \omega_- \cos \phi - (\tilde{\alpha}_+ + \tilde{\alpha}_-) \omega_- \sin \phi]. \end{aligned} \quad (19)$$

The dc voltage then follows from substitution into Eq. (17),

$$V = \frac{m_0|J_0|^2 g_- G_-(g_1 + G_1)}{eG_1 g_1 g_{1+} G_{1+} |f(\omega)|^2} \{ \omega^2 (2\omega_+ \tilde{\alpha}_+ + \omega_+ \tilde{\alpha}_- + \omega_- \tilde{\alpha}_- \cos \phi) - \omega_- [(1 + \tilde{\alpha}_+^2 + \tilde{\alpha}_+ \tilde{\alpha}_-) \omega^2 + \omega_-^2 - \omega_+^2] \sin \phi \}. \quad (20)$$

In the limit $\tilde{\alpha}_\pm \ll 1$ (which is appropriate for most experiments), Eq. (20) simplifies to the asymmetric Lorentzian

$$V = V_0 \frac{\omega_0^2 - (\omega - \omega_0)\delta'}{(\omega - \omega_0)^2 + \delta^2}, \quad (21)$$

with

$$V_0 = \frac{m_0|J_0|^2 g_- G_-(g_1 + G_1)}{4\omega_0^2 eG_1 g_1 g_{1+} G_{1+}} (2\omega_+ \tilde{\alpha}_+ + \omega_+ \tilde{\alpha}_- + \omega_- \tilde{\alpha}_- \cos \phi), \quad (22)$$

and

$$\begin{aligned} \omega_0^2 &= \omega_+^2 - \omega_-^2, \\ \delta &= \tilde{\alpha}_+ \omega_+ + \tilde{\alpha}_- \omega_- \cos \phi, \\ \delta' &= \frac{2\omega_0 \omega_- \sin \phi}{2\omega_+ \tilde{\alpha}_+ + \omega_+ \tilde{\alpha}_- + \omega_- \tilde{\alpha}_- \cos \phi}. \end{aligned} \quad (23)$$

The asymmetry of the lineshape (21) depends on the anisotropy of the torque τ_{eq} and on the angle $\phi/2$ between the principal axes and the direction \mathbf{n} of the magnetization of the fixed layer. In the experiment of Ref. 11 the main contribution to τ_{eq} comes from the large magnetic field used to align the free layer magnetization perpendicular to \mathbf{n} . This contribution is isotropic, which explains why no strongly asymmetric lineshapes were observed in Ref. 11. The experiment of Ref. 10 finds a significantly asymmetric lineshape if the applied magnetic field is small, the lineshapes becoming more symmetric at larger fields, consistent with our theory. (Reference 10 attributes the asymmetric lineshape to the imaginary part g_2 of the mixing conductance which, if large enough, provides another mechanism for an asymmetric lineshape, see the discussion below.)

The relative contributions of the rectification and the spin emission effects can be found by looking at the ratio of $m_0 \langle J m_1 \rangle / e$ and $\langle \dot{m}_2 m_1 \rangle \tilde{\alpha}_-$, *cf.* Eq. (17). For $\tilde{\alpha}_\pm \ll 1$ this ratio is

$$\frac{m_0 \langle J m_1 \rangle}{e \langle \dot{m}_2 m_1 \rangle \tilde{\alpha}_-} = -2 \frac{\delta - \omega_- \sin \phi (\omega - \omega_0) / \omega_0}{\tilde{\alpha}_- (\omega_+ - \omega_- \cos \phi)}. \quad (24)$$

Since both terms in the numerator are of order δ near the ferromagnetic resonance, whereas the denominator is of order $\tilde{\alpha}_- \omega_0$, the ratio (24) is of order $\delta / \tilde{\alpha}_- \omega_0$. This is of order unity if $\tilde{\alpha}_+$ and $\tilde{\alpha}_-$ are comparable, which happens precisely if the second term in Eq. (15) is not small in comparison to the first. This, in turn, is the condition that spin emission gives a significant contribution to the total damping. Hence, we conclude that spin emission contributes significantly to the measured dc voltage if and only if spin emission contributes significantly to the damping. Since $\langle \dot{m}_2 m_1 \rangle$ is symmetric around $\omega = \omega_0$, *cf.*

Eq. (19) above, spin emission contributes to the symmetric part of the lineshape only. The antisymmetric part is due to the rectification of the applied ac current only.

In our calculations we have neglected the imaginary parts g_2 and G_2 of the mixing conductance because in metallic junctions they are known to be numerically small in comparison to the real parts g_1 and G_1 . Inclusion of g_2 and G_2 leads to a small modification of the resonance frequency, because g_2 and G_2 change the gyromagnetic ratio γ of the free ferromagnetic layer.¹² With corrections to first order in g_2/g_1 only, the resonance frequency becomes

$$\begin{aligned} \omega_0^2 &= (\omega_+^2 - \omega_-^2) \\ &\times \left[1 - \frac{4\tilde{\alpha}_- g_2 (g_1 G_{1+} + 2G_1 G_{1+} - G_1 G_+) }{g_1 (G_1 G_+ + g_1 G_+ - g_1 G_{1+})} \right]. \end{aligned} \quad (25)$$

More importantly, with nonzero g_2 and G_2 , there is a finite asymmetry in the lineshape even in the absence of magnetic anisotropy in the free layer,¹⁰

$$\delta' = \frac{2\omega_0 [\omega_- \sin \phi - z(\omega_+ + \omega_- \cos \phi)]}{2\omega_+ \tilde{\alpha}_+ + \omega_+ \tilde{\alpha}_- + \omega_- \tilde{\alpha}_- \cos \phi - 2z\tilde{\alpha}_- \omega_- \sin \phi}, \quad (26)$$

with

$$z = \frac{G_1^2 g_{1+} g_2 G_- - 2g_1^2 G_{1+} G_2 g_-}{g_1 G_1 (g_1 + G_1) g_{1+} G_-}. \quad (27)$$

Again, our results are valid up to first order in g_2/g_1 and G_2/G_1 only.

We have also analyzed the case that the equilibrium angle between the fixed layer magnetization \mathbf{n} and the free layer magnetization \mathbf{m} is not 90 degrees. While this complicates the detailed expression for $V_{\text{dc}}(\omega)$ (to the extent that it cannot be reported here), it does not change our qualitative conclusions that (i) spin emission and rectification of the applied ac current have comparable contributions to the generated dc voltage if the free layer is thin enough that spin emission gives a sizable enhancement of the damping and (ii) the asymmetry of $V_{\text{dc}}(\omega)$

around the resonance frequency ω_0 is small in the ratios ω_-/ω_+ or g_2/g_1 . The former ratio is small if the applied magnetic field is large enough to saturate the free ferromagnet, whereas the latter ratio g_2/g_1 is known to be numerically small for metallic junctions (of order 0.1 or less, see Refs. 17,19,20) .

V. CONCLUSION

In this article we have presented a microscopic theory for the spin-torque driven ferromagnetic resonance in ferromagnet–normal-metal–ferromagnet trilayers. Our theory is inspired by the experiments of Refs. 10 and 11. In these experiments, an alternating current is used to drive the ferromagnetic resonance, while a generated dc voltage is used to detect the resonance.

In addition to providing theoretical expressions for the width and asymmetry of the resonance, we are able to determine the relative magnitude of two physical mechanisms that contribute to the dc voltage: rectification of the applied ac current and rectification of the spin currents emitted by the precessing ferromagnet. Both contributions are of similar magnitude for the thin ferromagnetic films used in the experiments. The presence of two mechanisms to generate a direct response to periodic driving, rather than one, sets this class of magnetic devices apart from their semiconductor counterparts.

A direct experimental probe of the two contributions

to the dc voltage is to compare the dc voltage observed in spin-torque driven ferromagnetic resonance with the dc voltage generated in conventional magnetic-field driven ferromagnetic resonance in the same device. The latter follows from rectification of emitted spin currents only. Since spin emission gives a symmetric line shape around the resonance frequency $\omega = \omega_0$ there should be a clear difference between the two methods to excite ferromagnetic resonance. A comparison of the magnitudes of both contributions would require a calibration of the amplitude at which the magnetization precesses. This can be achieved through a simultaneous measurement of the dc resistance of the device, which depends on the precession amplitude through the giant magnetoresistance effect.

Acknowledgments

We thank D. Ralph and J. Sankey for stimulating discussions. This work was supported by the Cornell Center for Materials research under NSF grant no. DMR 0520404, the Cornell Center for Nanoscale Systems under NSF grant no. EEC-0117770, by the NSF under grant no. DMR 0334499, and by the Packard Foundation. Upon completion of this manuscript we learned of a work by A. A. Kovalev, G. E. W. Bauer, and A. Brataas with similar conclusions about spin-torque driven ferromagnetic resonance.²⁴ We thank Alex Kovalev for sending us a preprint of this work.

¹ J. C. Slonczewski, *J. Magn. Magn. Mater.* **159**, 1 (1996).
² L. Berger, *Phys. Rev. B* **54**, 9353 (1996).
³ M. Tsoi, A. G. M. Jansen, J. Bass, W.-C. Chiang, M. Seck, V. Tsoi, and P. Wyder, *Phys. Rev. Lett.* **80**, 4281 (1998).
⁴ J. Z. Sun, *J. Magn. Magn. Mater.* **202**, 157 (1999).
⁵ J.-E. Wegrowe, D. Kelly, Y. Jaccard, P. Guittienne, and J.-P. Ansermet, *Europhys. Lett.* **45**, 626 (1999).
⁶ E. Myers, D. Ralph, J. Katine, R. Louie, and R. Buhrman, *Science* **285**, 867 (1999).
⁷ J. A. Katine, F. J. Albert, R. A. Buhrman, E. B. Myers, and D. C. Ralph, *Phys. Rev. Lett.* **84**, 3149 (2000).
⁸ Y. Tserkovnyak, A. Brataas, G. E. W. Bauer, and B. I. Halperin, *Rev. Mod. Phys.* **77**, 1375 (2005).
⁹ A. Brataas, G. E. W. Bauer, and P. J. Kelly, *Phys. Rep.* **427**, 157 (2006).
¹⁰ A. A. Tulapurkar, Y. Suzuki, A. Fukushima, H. Kubota, H. Maehara, K. Tsunekawa, D. D. Djayaprawira, N. Watanabe, and S. Yuasa, *Nature* **438**, 339 (2005).
¹¹ J. C. Sankey, P. M. Braganca, A. G. F. Garcia, I. N. Krivorotov, R. A. Buhrman, and D. C. Ralph, *Phys. Rev. Lett.* **96**, 227601 (2006).
¹² Y. Tserkovnyak, A. Brataas, and G. E. W. Bauer, *Phys. Rev. Lett.* **88**, 117601 (2002).
¹³ X. Waintal, E. B. Myers, P. W. Brouwer, and D. C. Ralph, *Phys. Rev. B* **62**, 12317 (2000).
¹⁴ M. D. Stiles and A. Zangwill, *Phys. Rev. B* **66**, 014407 (2002).
¹⁵ A finite resistance of the normal-metal spacer layer can be taken into account by making the replacements $G_+ \rightarrow 2G_N(G_N G_+ + G_+^2 - G_-^2)/((G_N + G_+)^2 - G_-^2)$, $G_- \rightarrow 2G_N^2 G_-/((G_N + G_+)^2 - G_-^2)$, $G_1 \rightarrow G_N(G_1^2 + G_1 G_N + G_+^2)/((G_1 + G_N)^2 + G_+^2)$, and $G_2 \rightarrow G_N^2 G_2/((G_1 + G_N)^2 + G_+^2)$ in the equations below, where G_N is the conductance of the normal metal (per spin direction). A finite resistance of the free ferromagnetic layer can be taken into account by making the replacements $1/g_\uparrow \rightarrow 1/g_\uparrow + 1/2g_{F\uparrow}$, $1/g_\downarrow \rightarrow 1/g_\downarrow + 1/2g_{F\downarrow}$, with $g_\pm = (g_\uparrow \pm g_\downarrow)/2$, while keeping g_1 and g_2 unchanged. Here $g_{F\uparrow}$ and $g_{F\downarrow}$ are the majority and minority conductances of the ferromagnet. In all cases, contact resistances should be excluded from the conductances.
¹⁶ A. Brataas, Y. V. Nazarov, and G. E. W. Bauer, *Phys. Rev. Lett.* **84**, 2481 (2000).
¹⁷ K. Xia, P. J. Kelly, G. E. W. Bauer, A. Brataas, and I. Turek, *Phys. Rev. B* **65**, 220401(R) (2002).
¹⁸ S. Adam, M. L. Polianski, and P. W. Brouwer, *Phys. Rev. B* **73**, 024425 (2006).
¹⁹ M. Zwierzycki, Y. Tserkovnyak, P. J. Kelly, A. Brataas, and G. E. W. Bauer, *Phys. Rev. B* **71**, 064420 (2005).
²⁰ M. A. Zimmler, B. Özyilmaz, W. Chen, A. D. Kent, J. Z. Sun, M. J. Rooks, and R. H. Koch, *Phys. Rev. B* **70**, 184438 (2004).
²¹ E. M. Lifshitz and L. P. Pitaevskii, *Statistical Physics, part 2* (Pergamon, 1980).
²² T. L. Gilbert, *IEEE Trans. Mag.* **40**, 3443 (2004).
²³ R. C. O’Handley, *Modern Magnetic Materials* (Wiley (New

²⁴ York), 2000).
(2006).
A. A. Kovalev, G. E. W. Bauer, and A. Brataas, preprint